Two-angle model and phase diagram for chromatin

Philipp M. Diesinger and Dieter W. Heermann
Institut für Theoretische Physik, Universität Heidelberg, Philosophenweg 19, D-69120 Heidelberg, Germany
and Interdisziplinäres Zentrum für Wissenschaftliches Rechnen der Universität Heidelberg, Heidelberg, Germany
(Received 3 May 2005; revised manuscript received 10 November 2006; published 8 September 2006)

We have studied the phase diagram for chromatin within the framework of the two-angle model. Only a rough estimation of the forbidden surface of the phase diagram for chromatin was given in a previous work of Schiessel. We revealed the fine structure of this excluded-volume borderline numerically and analytically. Furthermore, we investigated the Coulomb repulsion of the DNA linkers to compare it with the previous results.

DOI: 10.1103/PhysRevE.74.031904 PACS number(s): 87.15.Aa

I. INTRODUCTION

The basic repeat unit of the chromatin fiber [1] of all eucaryotic organisms is the so-called nucleosome, which consists of a cylindrical shaped histone complex and a stretch of DNA. This DNA stretch is wrapped around the histone disks approximately two times and connects them with each other. The histone complex consists of four pairs of core histones (H2A, H2B, H3, and H4) and is known up to atomistic resolution [2]. The nucleosomes form the next level of DNA compaction which is called the chromatin or 30-nm fiber.

The degree of compaction depends on the salt concentration [3] and on the presence of linker histones [4]. The presence of the linker histones leads to the formation of stemlike structures which are formed by the in- and outcoming DNA string. At low salt concentration a 10-nm structure is formed which has the shape of beads on a string [3], whereas at high salt concentrations the chromatin fiber is much more compact and has a diameter of 30 nm [5].

The chromatin structure is still not completely understood [1,6,7]. There are two competing models for its structure: The crossed-linker models [4,8–10] and the solenoid models [3,11,12]. In the case of the crossed-linker models the DNA linkers between the histone complexes are straight and consecutive nucleosomes sit on opposite sides of the chromatin fiber whereas in the case of the solenoid models one assumes that the linker DNA is bent and the nucleosomes form a helix. The chromatin fiber has been investigated by electron cryomicroscopy [4,13], atomic force microscopy [14,15], neutron scattering, and scanning transmission electron microscopy [16].

The two-angle model (see the next section) was introduced by Woodcock *et al.* [8] to describe the geometry of the 30-nm chromatin fiber. It has been shown that the excluded volume of the histone complex plays a very important role for the stiffness of the chromatin fiber [17] and for the topological constraints during condensation and decondensation processes [18]. In Ref. [19] a rough approximation of the forbidden surface in the chromatin phase diagram was given. In this work we want to answer the still open question of the fine structure of the excluded volume borderline which separates the allowed and forbidden states in the phase diagram. We revealed this borderline with simulations and analytical methods and the results of these two approaches are in very good agreement.

II. TWO-ANGLE MODEL

We will give some basic equations and a proper mathematical definition for the two-angle model in this section. Equations (1)–(6) will be used in the next part, where we will calculate the fine structure of the forbidden surface in the chromatin phase diagram.

The two-angle model describes the chromatin structure at the 30-nm scale by the following three parameters: the entry-exit angle α, the rotational angle β, and the linker length b (cf. Fig. 1). Let us consider four consecutive nucleosome locations (cf. Fig. 1): N_0, N_1, N_2, and $N_3 \epsilon \mathbb{R}^3$ within the fiber: If N_0, N_1, and N_2 are given then the next nucleosome location N_3 is determined by fulfilling the following conditions:

(i) $\sphericalangle((N_0-N_1),(N_2-N_1))=\alpha$;

(ii) $\|N_2-N_1\|=b_2$, $\|N_0-N_1\|=b_1$, $\|N_3-N_2\|=b_3$, with $b_1,\ldots,b_3=b$;

(iii) $P:=\{r\epsilon\mathbb{R}^3 | \exists \lambda,\mu\epsilon\mathbb{R}$, such that $r=N_1+\lambda(N_0-N_1)+\mu(N_2-N_1)\}$ $P':=\{r\epsilon\mathbb{R}^3 | \exists \lambda',\mu'\epsilon\mathbb{R}$, such that $r=N_1+\lambda'(N_2-N_1)+\mu'(N_3-N_1)\}$ $\sphericalangle(P,P')=\beta$.

By straightforward considerations this leads to the following expression for N_3 in the dependence of N_0, N_1, and N_2:

$$N_3 = R_\beta^{\hat{w}} R_{\pi-\alpha}^{\hat{v}} \left(N_2 + b_3 \frac{(N_2-N_1)}{\|N_2-N_1\|} \right)$$

$$\hat{v} := \frac{(N_2-N_1)\times(N_0-N_1)}{\|(N_2-N_1)\times(N_0-N_1)\|}; \quad \hat{w} := \frac{N_1-N_2}{\|N_1-N_2\|},$$

where $\|N_2-N_1\|=b_2$ and R_φ^v is the orthogonal rotational transformation matrix defined by the axis $v\epsilon\mathbb{R}^3$ and the rotation angle $\varphi\epsilon[0,2\pi]$ (with respect to the right-hand rule).

Note that the chromatin fibers described by these equations do *not* show a tangential distance between the ingoing and the outcoming DNA linkers, which is a consequence of the H1 histone stems in real chromatin fibers. Furthermore, this geometrical model assumes *straight* linkers between consecutive nucleosome complexes. A more detailed look at the two-angle model is provided by Schiessel in Ref. [19].

He also showed that for every ideal chromatin fiber with a certain set of values (α, β, b) it is possible to construct a spiral with radius R and a gradient m so that all the nucleosomes are located on this spiral. The parametrization of the spiral is

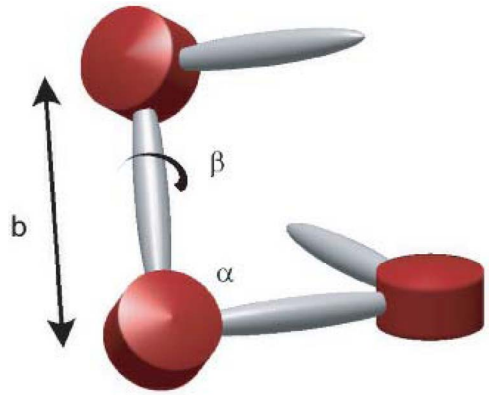

FIG. 1. (Color online) Basic definitions of the two-angle model: The entry-exit angle α, the linker length b, and the rotational angle β. The cylinders represent the nucleosomes.

$$\gamma(t) := \begin{pmatrix} R\cos\left(\frac{at}{R}\right) \\ R\sin\left(\frac{at}{R}\right) \\ t \end{pmatrix}, \quad t\epsilon\mathbb{R},$$

where R is the radius and $m=\frac{1}{a}$ is the gradient of this master solenoid. The distance between two consecutive nucleosomes along the z axis will be denoted by d in the following.

Furthermore, Schiessel showed in his work the following three equations, which relate R, a, and d to α, β, and b and thus the *global* fiber geometry to these *local* variables:

$$b^2 = 2R^2\left[1-\cos\left(\frac{ad}{R}\right)\right] + d^2, \tag{1}$$

$$\cos(\pi-\alpha) = \frac{2R^2\cos\left(\frac{ad}{R}\right)\left[1-\cos\left(\frac{ad}{R}\right)\right] + d^2}{2R^2\left[1-\cos\left(\frac{ad}{R}\right)\right] + d^2}, \tag{2}$$

$$\cos(\beta) = \frac{d^2\cos\left(\frac{ad}{R}\right) + R^2\sin^2\left(\frac{ad}{R}\right)}{d^2 + R^2\sin^2\left(\frac{ad}{R}\right)}. \tag{3}$$

The inverse transformation will be very useful, too:

$$R = \frac{b\cos\left(\frac{\alpha}{2}\right)}{2\left[1-\sin^2\left(\frac{\alpha}{2}\right)\cos^2\left(\frac{\beta}{2}\right)\right]}, \tag{4}$$

$$m = \frac{2\sin\left(\frac{\beta}{2}\right)\sqrt{1-\sin^2\left(\frac{\alpha}{2}\right)\cos^2\left(\frac{\beta}{2}\right)}}{\cot\left(\frac{\alpha}{2}\right)\arccos\left[2\sin^2\left(\frac{\alpha}{2}\right)\cos^2\left(\frac{\beta}{2}\right)-1\right]}, \tag{5}$$

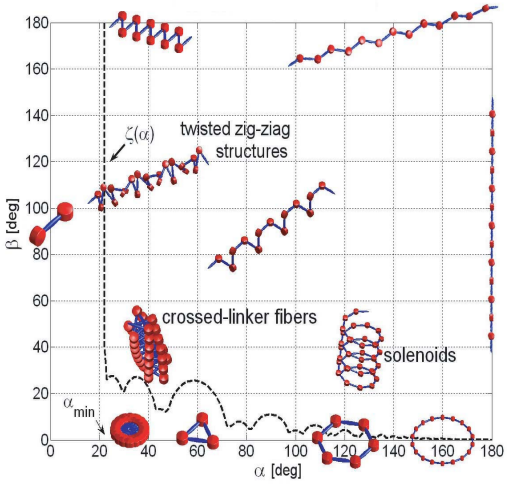

FIG. 2. (Color online) The chromatin phase diagram with some chromatin structures for different values of α and β. The solenoid and crossed-linker structures are most important. The dotted line is the function $\zeta(\alpha)$ which represents the border of the forbidden surface.

$$d = \frac{b\sin\left(\frac{\beta}{2}\right)}{\sqrt{\csc^2\left(\frac{\alpha}{2}\right)-\cos^2\left(\frac{\beta}{2}\right)}} \overset{\beta\ll 1}{\approx} \frac{b\beta}{2\sqrt{\csc^2\left(\frac{\alpha}{2}\right)-1}} + o(\beta)^3. \tag{6}$$

III. PHASE DIAGRAM

In this section the calculation of the fine structure of the excluded volume borderline is presented. Furthermore, we used a simple model to simulate the chromatin fiber: We used the two-angle model to generate chromatin fibers and then checked which states are the forbidden ones in the phase diagram. We assumed a spherical excluded volume (of radius 5 nm) and a linker length of 21 nm for both cases. Remember that the linker length b is the distance between the centers of the nucleosomes and not the "real" length of the linkers. At the end of this section the calculations and the simulational results are compared.

Figure 2 shows a picture of the chromatin phase diagram: Every set of angles (α,β) represents a particular structure in the two-angle model (the linker length b is considered to be constant). A detailed discussion of all possible structures and the phase diagram can be found in Ref. [19]. We will concentrate here on the case $\beta=0$ since it will turn out that these planar structures are very important for the calculation of the forbidden surface.

If $\alpha\approx\pi$, the fiber forms a circle [with radius $R\approx\frac{b}{\pi-\alpha}$ as follows from Eq. (4)]. Its radius converges towards infinity for $\alpha\to\pi$. For particular values of α the fiber forms *regular polygons*. For instance, the value $\alpha=\frac{\pi}{2}$ corresponds to the square and $\alpha=\frac{\pi}{3}$ is the regular triangle (cf. Fig. 2). To characterize these regular polygons one needs two variables: At

first the number of the tips i and second the number of loops the fiber needs to arrive at the starting point again, which we will call the "order" n of the polygon in the following.

These special values are given by

$$\alpha_i^n = \pi - \left(\frac{n2\pi}{i}\right), \quad \text{with } i,n \epsilon \mathbb{N} \quad \text{and } i \geq 2n, \text{ such that}$$

$$\nexists n', i' \epsilon \mathbb{N} \quad \text{with } n' < n \quad \text{and } \alpha_i^n = \alpha_{i'}^{n'} (\triangle). \tag{7}$$

The order n of α_i^n is a measure of its influence on the forbidden surfaces of the excluded volume structure of the phase diagram. Therefore all different values of α_i^n have to be sorted by n first and second by i—this makes the condition ($\triangle$) necessary: For example, $\alpha_3^1 = \alpha_6^2 = \alpha_9^3$ but the order of these three α_i^n is always $n=1$ and therefore they are all in the same equivalence class (the special case $i=2n$ leads to one-dimensional structures with $\alpha_2^1 = 0$—this value α_i^n of highest order in n and i plays an important role for the forbidden area in the phase diagram and is therefore mentioned here, too). We will show that it is possible to characterize all peaks of the forbidden surface by these two parameters n and i. This classification is shown in Fig. 4.

The condition ($\triangle$) simply means that *n and i have to be coprime*. Remember that α_i^n depends only on the relation $\frac{n}{i}$. We give a proof of this equivalence in the Appendix:

$$(\triangle) \Leftrightarrow \nexists \alpha, \beta, b \in \mathbb{N} \quad \text{with } n = \alpha b \quad \text{and } i = \beta b (\star).$$

Now consider the case that n and n' are coprime with $n' > n$, $i \geq 2n$, and $i' \geq 2n'$ such that $\frac{n}{i}, \frac{n'}{i'} \notin \frac{1}{\mathbb{N}}$ (which means that they are not equivalent to any order-1-value of α_i^n). Furthermore, assume that $\frac{n'}{i'} = \frac{n}{i} \Rightarrow i' = \left(\frac{n'}{n}\right) i$, it is clear that $\left(\frac{n'}{n}\right) \notin \mathbb{N}$ and $i \in \mathbb{N}$, therefore $\exists \alpha \in \mathbb{N}$ so that $i = \alpha n$ which contradicts $\left(\frac{i}{n}\right) \notin \mathbb{N}$. This means that if two orders n_1 and n_2 are coprime with $n_1, n_2 > 1$, there are *never* equal values of $\alpha_i^{n_1}$ and $\alpha_{i'}^{n_2}$ for all possible $i \geq 2n$, $i' \geq 2n'$, and $i, i' \in \mathbb{N}$. For example, n and $n+1$ are always coprime numbers and therefore have never common α_i^n.

So for a given order n the possible values of α_i^n depend on the prime factor dismantling of n and therefore are very irregular. If n is a prime number, all $i \geq 2n$ with $i \notin n\mathbb{N}$ are allowed: For $n=2$ all $i \geq 4$ with $i \notin 2\mathbb{N}$ are allowed and for $n=3$ all i with $i \geq 2n$, $i \notin 3\mathbb{N}$ are allowed (and for $n=1$ all $i \geq 2$ are allowed). So between two values of α_i^1 there is one of α_i^2 and two of α_i^3.

The distances $\Delta_{i_1}^n = \alpha_{i_2}^n - \alpha_{i_1}^n$ between two consecutive $i_2 > i_1$ are given below for the first three and additional for all prime orders:

$$n = 1 : \alpha_i^1 = \pi - \frac{2\pi}{i}, \quad (i \geq 2n) \Rightarrow \Delta_i^1 = \frac{2\pi}{i(i+1)},$$

$$n = 2 : \alpha_i^2 = \pi - \frac{4\pi}{i}, \quad (i \geq 2n \quad \text{and } i \notin 2\mathbb{N}) \Rightarrow \Delta_i^2 = \frac{8\pi}{i(i+2)},$$

$$n = 3 : \alpha_i^3 = \pi - \frac{6\pi}{i}, \quad (i \geq 2n \quad \text{and } i \notin 3\mathbb{N}) \Rightarrow \Delta_i^3 = \frac{\text{mod}(i,3) 6\pi}{i[i + \text{mod}(i,3)]},$$

$$n \text{ prime} : \alpha_i^n = \pi - \frac{n2\pi}{i}, \quad (i \geq 2n \quad \text{and } i \notin n\mathbb{N}) \Rightarrow \Delta_i^n = \frac{mn2\pi}{i(i+m)}, \quad m = \begin{cases} 1 & \text{if mod}(i,n) < n-1 \\ 2 & \text{if mod}(i,n) = n-1 \end{cases}.$$

Furthermore, this shows that the distances $\Delta_i^n \overset{n \to \infty}{\to} 0$, because the counter is always $\sim n$ and the leading term of the denominator is at least $\sim n^2$ (remember $i > 2n$).

The most interesting structures of the chromatin phase diagram are the following two cases: solenoidlike structures and fibers with crossed linkers. An extensive discussion of these two structures can be found in Ref. [19] and here a short overview will be given since we need some basic equations of these structures for our further calculations.

For small $\beta \ll 1$ and $\alpha \approx \pi$ the chromatin fibers resemble solenoids. The condition $\left(\frac{da}{R}\right) \ll 1$ and Eqs. (1)–(3) lead to the geometrical properties of the solenoidlike fibers: The radius of the fiber is r and l_N is the length of a fiber of N monomers [19]:

$$r = \frac{b(\pi - \alpha)}{\beta^2 + (\pi - \alpha)^2}, \quad l_N = \frac{bN\beta}{\sqrt{\beta^2 + (\pi - \alpha)^2}}.$$

The vertical distance δ between two loops plays an important role in the following sections. It can be obtained by $\delta \approx l \frac{2\pi}{\pi - \alpha}$, which leads to

$$\delta \approx \frac{\left(\frac{2\pi}{\pi - \alpha}\right) b\beta}{\sqrt{\beta^2 + (\pi - \alpha)^2}}. \tag{8}$$

One can also calculate the exact value of δ by

$$\delta = \int_{t=0}^{2\pi r/a} m(\gamma(t)) |(\gamma_x'(t), \gamma_y'(t))^t| dt = \frac{4b\pi \sin(\alpha/2) \sin(\beta/2)}{\arccos[2\cos^2(\beta/2)\sin^2(\alpha/2) - 1] \sqrt{3 + \cos(\alpha) + [\cos(\alpha) - 1]\cos(\beta)}}.$$

However, the approximation (8) is much more useful.

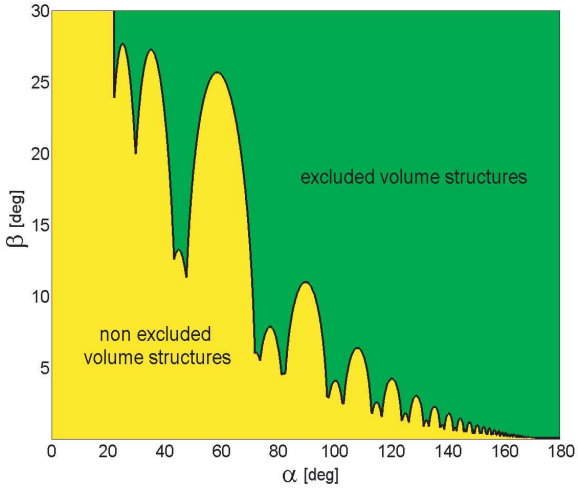

FIG. 3. (Color online) Fine structure of the excluded-volume "phase transition." The chromatin fibers beneath the borderline fulfill the excluded volume conditions, those above do not. The borderline is the function $\zeta(\alpha)$.

Now let us consider the crossed-linker fibers. Consider the case $\beta \ll 1$ and $\alpha \ll \pi$: Above the regular polygons have been discussed. For a nonvanishing β these regular polymers open up in an accordionlike manner. This leads to three-dimensional fibers with crossed linkers (cf. Fig. 2). Using $\beta \ll 1$ and Eqs. (1)–(3) one gets (cf. Ref. [19])

$$r = \frac{b}{2\cos(\alpha/2)}\left[1 - \frac{\beta^2}{4}\cot^2\left(\frac{\pi-\alpha}{2}\right)\right],$$

$$l_N = \frac{N\beta b}{2}\cot\left(\frac{\pi-\alpha}{2}\right).$$

Now δ follows again from $\delta \approx l\frac{2\pi}{\pi-\alpha}$:

$$\delta \approx \frac{1}{2}\left(\frac{2\pi}{\pi-\alpha}\right)\beta b \tan\left(\frac{\alpha}{2}\right). \tag{9}$$

Now we will turn to the calculation of the forbidden surface of the chromatin phase diagram. It will turn out that the excluded-volume borderline, which separates the forbidden states from the allowed ones, is a function of α. We will call it ζ and calculate it in the following part of this section. This borderline is shown in Fig. 2 as a dashed line, too. The interesting part of the phase diagram for the excluded-volume phase transition is the lower one with $\beta \in [0°, 30°]$. This cutout of the phase diagram is shown in Fig. 3.

Every "peak" of ζ corresponds to a regular polygon: The large peaks correspond to polygons of order 1 and the smaller ones to order 2 and order 3 polygons. Between two order-1 peaks there is one order-2 peak and two order-3 peaks. The classification of these peaks is shown in Fig. 4: ζ has local maxima at every α_i^n.

The planar structures which belong to $(\alpha_i^n, \beta=0)$ need a large rise of β to arrive in the area of the excluded volume structures, because at $\beta=0$ nucleosome k and $k+\frac{n2\pi}{\pi-\alpha_i^n}$ are

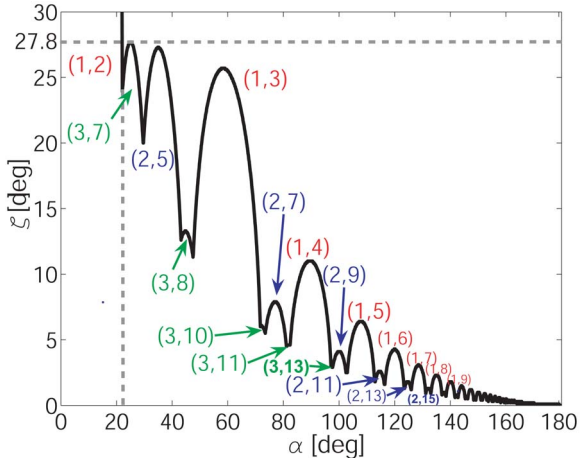

FIG. 4. (Color online) Excluded volume borderline and the classification of its peaks.

located exactly at the same position. At first, consider only the special values α_i^n: At first order increasing β from 0 to some value $\tilde{\beta}$ leads to a vertical movement $\Delta_i^n(\tilde{\beta})$ of the relevant nucleosomes k and $k+\frac{n2\pi}{\pi-\alpha_i^n}$ along the chromatin axis. Assuming a spherical hard-core excluded volume of radius r for the nucleosomes we get $\Delta_i^n(\tilde{\beta}) = d \Rightarrow \zeta(\alpha_i^n) = \tilde{\beta}$.

For large α, $\Delta_i^n(\tilde{\beta})$ can be calculated by Eq. (8) and one finds

$$\Delta_i^n(\tilde{\beta}) = \frac{n\left(\frac{2\pi}{\pi-\alpha_i^n}\right)b\tilde{\beta}}{\sqrt{\tilde{\beta}^2 + (\pi-\alpha_i^n)^2}}; \tag{10}$$

with $\beta > 0$ this leads to

$$\tilde{\beta}_i^n(\Delta_i^n) = \sqrt{\frac{(\Delta_i^n(\pi-\alpha_i^n))^2}{b^2n^2\left(\frac{2\pi}{\pi-\alpha_i^n}\right)^2 - (\Delta_i^n)^2}} \tag{11}$$

and, furthermore, $\tilde{\beta}_i^n(d) = \zeta(\alpha_i^n)$ implies

$$\zeta(\alpha_i^n) = \sqrt{\frac{d^2(\pi-\alpha_i^n)}{b^2n^2\left(\frac{2\pi}{\pi-\alpha_i^n}\right)^2 - d^2}}. \tag{12}$$

Figure 5 shows the numerically calculated ζ function and the theoretical predictions for the maxima. As Eq. (10) shows, $\Delta_i^n(\tilde{\beta}) \sim n$. This means that planar structures at an α_i^n of *higher* order need a *smaller* rise of β to fulfill the excluded volume conditions and therefore ζ is decreasing with increasing α. In fact this is the reason why n is called the *order* of the peaks of ζ. It can be easily understood if one remembers the fact that a higher order means more nucleosomes are located between two overlapping ones. And thus a rise of β has a stronger effect than at lower orders.

As $\Delta_i^n(\tilde{\beta}) \to 0$ for $\alpha_i^n \to \pi$ the maxima of ζ converge towards 0 for $\alpha_i^n \to \pi$. There are infinitely many α_i^n for $n \to \infty$ and the distance Δ_i^n converges to zero, so ζ has infinitely

many local maxima and minima for $\alpha_i^n \to \pi$. It is clear that $\zeta(\pi)=0$ as the fiber forms a fully stretched fiber (a circle of radius $r=\infty$). This explains the forbidden strip at the left side of the figures as the maximum of highest order $(1,2)$ with a corresponding one-dimensional structure.

So far, ζ is only known at the positions of the maxima α_i^n. Now consider values of α, which are close to an α_i^n, say $\alpha' = \alpha_i^n \pm \Delta\alpha$ ("close" means such $\Delta\alpha$ which lead to a shift $\Delta a < 2r$). This leads to a slight shift Δa of those nucleosomes which are located at the same places [namely, k and $k + \left(\frac{n2\pi}{\pi-\alpha}\right)$]. At $\beta=0$ this shift Δa is orthogonal to the fiber's axis. This time Δ_i^n still denotes the distance between the nucleosomes k and $k+\left(\frac{n2\pi}{\pi-\alpha}\right)$ along the fiber's axis, but now they are not located at the same spots but slightly shifted. Therefore their distance Δ is no longer equal to their distance Δ_i^n along the axis, when increasing β.

In this case increasing β still leads to a movement along the vertical axis of the fiber, but now the distance Δ of nucleosome k and $k+\left(\frac{n2\pi}{\pi-\alpha}\right)$ increases like $\Delta^2 \approx \Delta a^2 + (\Delta_i^n)^2$. The fiber fulfills excluded volume, when $\Delta = 2r$, which means

$$\Delta_i^n = \sqrt{4r^2 - \Delta a^2} < 2r.$$

So the critical value of Δ_i^n, which has to be achieved to fulfill excluded volume, decreases with increasing Δa. Therefore ζ has a local maximum at α_i^n: $\zeta(\alpha_i^n \pm \Delta\alpha) < \zeta(\alpha_i^n)$.

To calculate $\Delta a_{i,n}$ in dependence of $\Delta\alpha$ imagine a planar structure of j nucleosomes with an entry-exit angle $\alpha' = \alpha_i^n \pm \Delta\alpha$ of two consecutive octamers. The locations of these nucleosomes are denoted by $p_0, p_1, p_2, \ldots, p_{j-1} \in \mathbb{R}^3$. Without loss of generality one can assume

$$p_0 = \begin{pmatrix} 0 \\ 0 \\ 0 \end{pmatrix}, \quad p_1 = \begin{pmatrix} b & \cos\left(\frac{\alpha'}{2}\right) \\ b & \sin\left(\frac{\alpha'}{2}\right) \\ 0 \end{pmatrix} \text{ and}$$

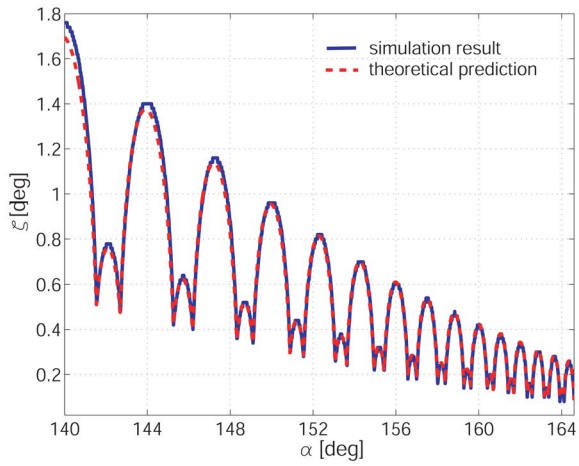

FIG. 5. (Color online) Calculated theoretical prediction (dashed line) and the simulation result (solid line) for the excluded volume borderline of the chromatin phase diagram.

$$\forall k \geq 2 : p_k = p_{k-1} + R(p_{k-1} - p_{k-2})$$

$$\text{with } R := R^z_{\pi-\alpha'} = \begin{pmatrix} \cos(\pi-\alpha') & \sin(\pi-\alpha') & 0 \\ -\sin(\pi-\alpha') & \cos(\pi-\alpha') & 0 \\ 0 & 0 & 1 \end{pmatrix}$$

the rotational matrix along the z axis. This leads to

$$p_k = \sum_{m=0}^{k-1} R^m p_1 \quad \forall k > 0.$$

Now $\Delta a_{i,n}$ is given by $\Delta a_{i,n} = \|p_{k=i}\|$, which leads to

$$\Delta a_{i,n} = \left\| \sum_{m=1}^{i} R^{m-1} p_1 \right\| \tag{13}$$

(where R and p_1 depend on i, n, and $\Delta\alpha$). Now one can use Eq. (11) to calculate ζ around the maximal values α_i^n:

$$\frac{n\left(\frac{2\pi}{\pi-\alpha'}\right) b\zeta(\alpha')}{\sqrt{\zeta(\alpha')^2 + (\pi-\alpha')^2}} \stackrel{!}{=} \sqrt{4r^2 - \Delta a^2} \stackrel{\zeta>0}{\Rightarrow} \zeta(\alpha' = \alpha_i^n \pm \Delta\alpha) = \sqrt{\frac{\left(4r^2 - \left\| \sum_{m=1}^{i} R^{m-1} p_1 \right\|^2\right)(\pi-\alpha')^2}{b^2 n^2 \left(\frac{2\pi}{\pi-\alpha'}\right)^2 - 4r^2 + \left\| \sum_{m=1}^{i} R^{m-1} p_1 \right\|^2}}. \tag{14}$$

Similar to the case of large α one can find equations for ζ of small α: In this case Eq. (9) leads to

$$\Delta_i^n(\tilde{\beta}) = \frac{1}{2} n \left(\frac{2\pi}{\pi-\alpha'}\right) \tilde{\beta} b \tan\left(\frac{\alpha'}{2}\right)$$

with $\alpha' = \alpha_i^n \pm \Delta\alpha$. Now again $\zeta(\alpha')$ follows from $\tilde{\beta}(\Delta_i^n = \sqrt{4r^2 - \Delta a_{i,n}^2}) = \zeta(\alpha')$:

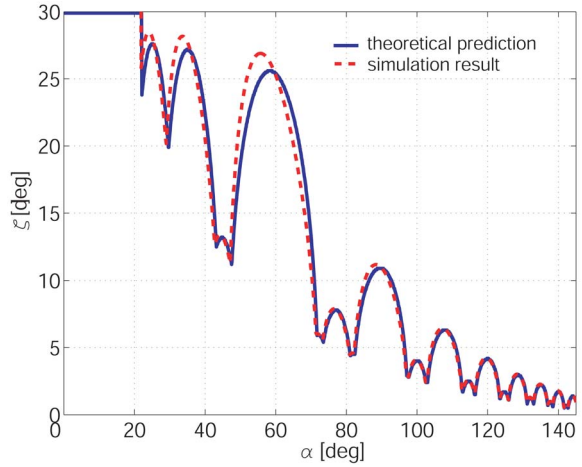

FIG. 6. (Color online) Calculated theoretical prediction (solid line) and the simulation result (dashed line) for the excluded volume borderline of the chromatin phase diagram.

$$\Rightarrow \zeta(\alpha' = \alpha_i^n \pm \Delta\alpha) = \frac{\cot\left(\frac{\alpha'}{2}\right)}{n\left(\frac{2\pi}{\pi - \alpha'}\right)b} \sqrt{4r^2 - \left\| \sum_{m=1}^{i} R^{m-1} p_1 \right\|^2}. \tag{15}$$

$|\Delta\alpha| < c$ fulfilling $\Delta a(c) = 2r$ gives the interval of the allowed α values: $\alpha' \in [\alpha_i^n - c, \alpha_i^n + c]$ for a certain peak (n,i).

The predictions of Eqs. (14) and (15) are shown in Figs. 5 and 6 together with our simulation results.

IV. EXCLUDED VOLUME RESTRICTIONS OF THE DNA LINKERS

As mentioned before the nucleosome-nucleosome excluded volume interactions are not the only ones within the chromatin fiber. The DNA linkers have a diameter of about 2 nm and therefore excluded volume restrictions, too. This is in particular very important for all crossed-linker structures. But since the DNA linkers have a very strong (although screened) Coulomb repulsion their excluded volume interactions can be revealed by looking at the Coulomb energy between the linkers. Other potentials like the nucleosome-nucleosome interaction or the interaction between DNA linkers and nucleosomes will be neglected here.

One can use the Debye-Hückel theory to model the Coulomb repulsion of the DNA linkers, but since the screening of this interaction starts at the radius of the DNA strand and due to the condensation of ions along the DNA linkers, one has to calculate a correction of the screened potential by fitting the tail of the Debye-Hückel potential for an infinitely long cylinder to the Gouy-Chapman potential in the far zone. This calculation can be found in Refs. [20,21] and leads to a corrected linear charge density ν_{eff} which is also given in the table above for different levels of monovalent salt concentration and can be found in Ref. [22], for instance. During the last two to three decades DNA models based on such potentials have been developed and applied widely, and their predictions are usually very good [23–29] (see Table I).

TABLE I. Screening of the Coulomb repulsion.

c_S [10^{-2} M]	1	2	3	4	5
κ [nm^{-1}]	0.330	0.467	0.572	0.660	0.738
ν_{eff} [e/nm]	−2.43	−2.96	−3.39	−3.91	4.15

So one can calculate the Coulomb repulsion between the DNA segments i and j by evaluating

$$V_{i,j} = \frac{\nu_{\text{eff}}}{c} \int\int \frac{e^{-\kappa r_{i,j}}}{r_{i,j}} dx_i dx_j, \tag{16}$$

where c is the total dielectric constant of water. These two integrals were numerically calculated and the results for the Coulomb energy of a single chromatin linker within a fiber is shown in Fig. 7.

One can see that the Coulomb repulsion of the linkers is very high within the gaps of the excluded volume borderline. The repulsion also diverges for the crossed linker fibers when β becomes too small.

V. DISCUSSION AND CONCLUSION

We used a spherical excluded volume to model the nucleosomes but since the radius (5 nm) and the height (6 nm) of the histone complex are nearly coincident this should be a suitable approximation. With a cylindrical excluded volume the peaks of the excluded volume borderline would show edges.

The DNA compaction plays a very important role for eucaryotic cells. Billions of base pairs have to fit into volumes with diameters of the order of a micron. The most compact, but still allowed, states are those close to the excluded volume borderline. A measurement [30] of the statistical distribution of the nucleosome repeat lengths indicates a value for

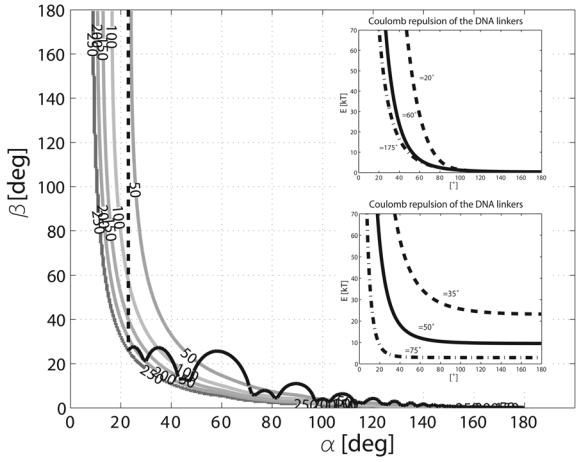

FIG. 7. Coulomb repulsion of the DNA linkers in kT. Shown are also two cuts in the inset.

β_{min} of 36° [9], but since chromatin fibers in living cells are strongly fluctuating, it is likely that short parts of the fiber can come very close to the excluded volume borderline or even use its gaps to contribute to the compaction of the whole genome. The cell might use this as a (further) statistical effect to achieve the strong compaction of the chromatin fiber.

We showed that the Coulomb repulsion of the DNA linkers is very high within the very compact states of the gaps of the excluded volume boderline, but one has to keep in mind that we neglected the internucleosomal interactions and the interactions between the linkers and the nucleosomes. Attractive potentials might reduce the total energy of these states again. Unfortunately the internucleosomal potential is not well known yet.

ACKNOWLEDGMENTS

We would like to thank Jörg Langowski, Lars Omlor, Jens Odenheimer, and Frank Aumann for the fruitful discussions.

APPENDIX

We will show here that the conditions ($\triangle$) and ($\star$) are equivalent: $\nexists n', i' \epsilon \mathbb{N}$ with $n' < n$ and $\alpha_i^n = \alpha_{i'}^{n'}$ ($\triangle$) $\Leftrightarrow \nexists \alpha, \beta, b \in \mathbb{N}$ with $n = \alpha b$ and $i = \beta b$($\star$).

"$\Rightarrow$" Let n be an arbitrary element of $\mathbb{N}$. Now assume that $i \in \mathbb{N}$, $i \geq 2n$ and n and i have a common divisor b, i.e., $\exists \alpha$, β, and $b \in \mathbb{N}$ such that $i = \alpha b$ and $n = \beta b \Rightarrow \frac{n}{i} = \frac{\beta b}{\alpha b} = \frac{\beta}{\alpha} = \frac{n/b}{i/b}$, furthermore, $i \geq 2n$ indicates $\frac{i}{b} \geq 2\frac{n}{b} \Rightarrow \frac{\beta}{\alpha} \leq \frac{1}{2}$ which means $\exists n', i' \epsilon \mathbb{N}$ with $i' \geq 2n'$ and $\frac{n'}{i'} = \frac{n}{i}$, namely, $n' = \beta$ and $i' = \alpha$. This means $\neg\star$ implies $\neg\triangle$ which is equivalent to $\triangle \Rightarrow \star$.

"$\Leftarrow$" To prove the other implication above it suffices to show that if n and i are coprime, there are no numbers m, j with $m < n$ such that $nj = mi$. Dividing this equation by $\gcd(n, m)$ one gets a new equation of the same structure with m' and n' instead of m and n, fulfilling $\gcd(m', n') = 1$. Moreover, $\gcd(n, i) = 1$ leads to $\gcd(n', i) = 1$. Thus $\gcd(m'i, n') = 1 \Rightarrow j = 1$ which contradicts to $j > 2n$.

The following effects have to be considered to explain the differences between the calculated theoretical predictions and the simulational results. The effective entry-exit angle α_e is the projection of α onto a plane which is orthogonal to the axis of the master solenoid. It decreases with increasing β. This is a consequence of the fact that the length of the fiber increases with increasing β. α_e is important for the calculation of the number of linkers which form a closed loop: $N_l = \frac{2\pi}{\pi - \alpha_e}$ ($\frac{2\pi}{\pi - \alpha_e}$ gives the number of breaks of α_e which has to be done to get a full loop. If $\frac{2\pi}{\pi - \alpha_e}$ is an integer, this is equal to the number of linkers, which corresponds to a full loop. If it is not an integer number, then the fractional part gives the fraction of $\pi - \alpha_e$ which is missing for a full loop, but the entry-exit angle is fixed here and it is assumed that $N_l = \frac{2\pi}{\pi - \alpha_e}$). In the calculations above $\alpha_e = \alpha = \text{const}$ was assumed, because only small β were considered. α_e will be calculated as a function of α and β below. It converges towards 0 for $\beta \to \pi$ for different values of α and β. To calculate α_e consider three consecutive nucleosome locations within a given fiber: n_0, n_1, and $n_2 \in \mathbb{R}^3$. Without loss of generality one can assume: $n_0 = p_0$, $n_1 = p_1 + p_0$, and $n_2 = p_2 + p_1 + p_0$ where the p_i are the following linker vectors:

$$p_0 = \begin{pmatrix} 0 \\ 0 \\ 0 \end{pmatrix}, \quad p_1 = \begin{pmatrix} \sqrt{b^2 - d^2} \\ 0 \\ d \end{pmatrix} \quad \text{and } p_2 = \begin{pmatrix} x_2 \\ y_2 \\ d \end{pmatrix}.$$

This means that the z axis of the coordinate system is the axis of the fiber [d is given by Eq. (6) and b is the linker length]. Now $\|p_2\| = b$ leads to

$$y_2 = \sqrt{b^2 - d^2 - x_2^2}$$

and x_2 can be calculated by using

$$\cos(\alpha) = \frac{\langle -p_1 | p_2 \rangle}{b^2} \Rightarrow x_2 = -\frac{b^2 \cos(\alpha) + d^2}{\sqrt{b^2 - d^2}}$$

with $d = \frac{b \sin(\beta/2)}{\sqrt{\csc^2(\alpha/2) - \cos^2(\beta/2)}}$; this leads to

$$y_2 = \sqrt{b^2 - d^2 - \frac{[b^2 \cos(\alpha) + d^2]^2}{b^2 - d^2}} \overset{d}{=} \sqrt{b^2 \cos^2\left(\frac{\beta}{2}\right) \sin^2(\alpha)}$$

and now α_e follows from the projection onto the x-y plane:

$$\frac{\sin(\alpha_e)}{2} = \frac{\sqrt{(x_1 + x_2)^2 + y_2^2}}{2\sqrt{x_2^2 + y_2^2}} \Rightarrow \sin\left(\frac{\alpha_e}{2}\right) = \sqrt{\frac{\cos(\beta/2)\sin^2(\alpha/2)}{2[1 + \cos(\alpha)]}}. \tag{A1}$$

As Eq. (A1) shows, α_e decreases with increasing β. As a consequence of this N_l decreases, too: If $\alpha_e \to 0$, then $N_l(\alpha, \beta) = \frac{2\pi}{\pi - \alpha_e(\alpha, \beta)} \to 2$. So all fibers with high values of beta need only approximately two nucleosomes for a complete loop. This is confirmed by Fig. 2. As α_e was assumed to be constant, N_l was also constant in the calculations above. This is a suitable approximation for small β. For larger β the assumed values of N_l were a bit too large and therefore the calculated values of ζ were a bit too small—but this effect is small compared to the other estimations which were made above. The error of ζ, due to the assumption that N_l is constant, increases with increasing β.

[1] K. E. van Holde, *Chromatin* (Springer-Verlag, New York, 1989).
[2] K. Luger, A. W. Mader, R. K. Richmond, D. F. Sargent, and T. J. Richmond, Nature (London) **389**, 251 (1997).
[3] F. Thoma, T. Koller, and A. Klug, J. Cell Biol. **83**, 403 (1979).
[4] J. Bednar *et al.*, Proc. Natl. Acad. Sci. U.S.A. **95**, 14173 (1998).
[5] J. Widom, J. Mol. Biol. **190**, 411 (1986).
[6] K. V. Holde and J. Zlatanova, J. Biol. Chem. **270**, 8373 (1995).
[7] K. V. Holde and J. Zlatanova, Proc. Natl. Acad. Sci. U.S.A. **93**, 10548 (1996).
[8] C. L. Woodcock, S. A. Grigoryev, R. A. Horowitz, and N. Whitaker, Proc. Natl. Acad. Sci. U.S.A. **90**, 9021 (1993).
[9] H. Schiessel, W. M. Gelbart, and Robijn Bruinsma, Biophys. J. **80**, 1940 (2001).
[10] B. Dorigo *et al.*, Science **306**, 1571 (2004).
[11] J. T. Finch and A. Klug, Proc. Natl. Acad. Sci. U.S.A. **73**, 1897 (1976).
[12] J. Widom and A. Klug, Annu. Rev. Biophys. Biophys. Chem. **43**, 207 (1985).
[13] J. Bednar, R. A. Horowitz, J. Dubochet, and C. L. Woodcock, J. Cell Biol. **131**, 1365 (1998).
[14] S. H. Leuba *et al.*, Proc. Natl. Acad. Sci. U.S.A. **91**, 11621 (1994).
[15] J. Zlatanova, S. H. Leuba, and K. van Holde, Biophys. J. **74**, 2554 (1998).
[16] S. E. Gerchman and V. Ramakrishhnan, Proc. Natl. Acad. Sci. U.S.A. **84**, 7802 (1987).
[17] B. Mergell, R. Everaers, and H. Schiessel, Phys. Rev. E **70**, 011915 (2004).
[18] M. Barbi *et al.*, Phys. Rev. E **71**, 031910 (2005).
[19] H. Schiessel, J. Phys.: Condens. Matter **15**, R699 (2003).
[20] J. Schellman and D. Stigter, Biopolymers **16**, 1415 (1977).
[21] D. Stigter, Biopolymers **16**, 1435 (1977).
[22] T. Schlick, A. D. Beard, J. Huang, D. A. Strahs, and X. Qian, Comput. Sci. Eng. **2**, 38 (2000).
[23] S. A. Allison and J. A. McCammon, Biopolymers **23**, 167 (1984).
[24] K. V. Klenin, M. D. Frank-Kamenetskii, and J. Langowski, Biophys. J. **68**, 1435 (1995).
[25] J. Delrow, J. A. Gebe, and J. M. Schurr, Biopolymers **42**, 455 (1997).
[26] K. Klenin, H. Merlitz, and J. Langowski, Biophys. J. **74**, 780 (1998).
[27] H. Merlitz, K. Rippe, K. V. Klenin, and J. Langowski, Biophys. J. **74**, 773 (1998).
[28] M. Hammermann, N. Brun, K. V. Klenin, R. May, K. Toth, and J. Langowski, Biophys. J. **75**, 3057 (1998).
[29] B. S. Fujimoto and J. M. Schurr, Biophys. J. **82**, 944 (2002).
[30] J. Widom, Proc. Natl. Acad. Sci. U.S.A. **89**, 1095 (1991).